New neighbours

I. 13 new companions to nearby M dwarfs[*]

X. Delfosse[1,2]**, T. Forveille**[1]**, J.-L. Beuzit**[2,3]**, S. Udry**[2]**, M. Mayor**[2]**, and C. Perrier**[1]

[1] Observatoire de Grenoble, Université J. Fourier, B.P. 53, F-38041 Grenoble, France
[2] Observatoire de Genève, CH-1290 Sauverny, Switzerland
[3] Canada-France-Hawaii Telescope Corporation, P.O. Box 1597, Kamuela, HI 96743, USA

Abstract. We present preliminary results of a long-term radial-velocity search for companions to nearby M dwarfs, started in September 95. The observed sample is volume-limited, and defined by the 127 northern ($\delta > -16°$) M dwarfs listed in the Gliese and Jahreiss (CNS3) catalogue with d≤9 pc and V≤15. Observations are obtained with the ELODIE spectrograph on the 1.93-m telescope of the Observatoire de Haute-Provence. The typical accuracy ranges between $10\,\mathrm{m\,s^{-1}}$ (the instrumental stability limit) for the brighter stars and $70\,\mathrm{m\,s^{-1}}$ at our limiting magnitude. We complement the ELODIE velocities with older measurements extracted from the CORAVEL database to extend our time base, albeit obviously with lower precision. Simultaneously, we perform adaptive optics imaging at CFHT and ESO to look for close ($a > 0.05$–$0.1''$) visual companions in a larger volume-limited sample. For stellar companions the two techniques together cover the full separation range, to beyond the limiting distance of the sample. We will therefore eventually obtain a statistically meaningful inventory of the stellar multiplicity of nearby M-dwarf systems. We also have useful sensitivity to giant planets, as illustrated by our recent detection of a planetary companion to Gl 876.

After 2.5 years, we have discovered 12 previously unknown components in this 127 stars sample, plus a companion to an additional star beyond its southern declination limit. 7 of these are actually beyond the 9 pc limit, as they belong to systems included in the sample on the basis of CNS3 photometric parallaxes which were biased-down by the unrecognized companion. The remaining 5 companions are true additions to the 9 pc inventory. More are certainly forthcoming, given our present selection bias towards short periods and relatively massive companions.

We have derived orbital elements for 7 of the new systems, as well as for some known binaries with previously undetermined orbits. One system, G 203-47, associates an M3.5V star with a white dwarf in a rather tight orbit ($a_1 \sin i = 15\,\mathrm{R_\odot}$) and represents a Post-Common-Envelope system. Some of the new M-dwarf binaries will over the next few years provide very precise mass determinations, and will thus better constrain the still poorly determined lower main-sequence mass-luminosity relation. The first such results are now being obtained, with some preliminary accuracies that range between 2% at 0.4–0.6 $\mathrm{M_\odot}$ and 10% at 0.1 $\mathrm{M_\odot}$. We have also discovered the third known detached M-dwarf eclipsing binary, and determined its masses with 0.4% accuracy.

Key words: instrumentation: adaptive optics – stars: binaries: spectroscopic – stars: binaries: visual – stars: low-mass, brown dwarfs – stars: planetary systems

1. Introduction

Binarity is a key observational parameter for many astrophysical questions. One particularly important issue is whether low mass stars and brown dwarfs significantly contribute to the dark matter in the galactic disk; the present uncertainties on the local mass function for very low mass stars are large enough for this question to be still unsettled (Tinney 1993), although evidence increasingly points towards a negative answer. The DENIS and 2MASS near infrared surveys will soon provide photometric luminosity functions with very good statistical precision, down to the brown-dwarf domain (Delfosse et al. 1997, 1998a; Kirkpatrick et al. 1997). The corrections for unresolved binaries and the mass-luminosity relation will then be the main uncertainty sources for the local stellar mass function. Below M∼0.3 $\mathrm{M_\odot}$, the mass-luminosity relation (Henry & McCarthy 1993) is only determined by few observational data points, most of which are of low accuracy. Accurate orbital elements are thus clearly needed for more low mass binaries, to provide additional direct stellar mass determinations. A better knowledge of the multiplicity statistics of low mass stars is also needed to account for the effect of unresolved systems on the mass and luminosity functions: at present, different plausible assumptions on stellar multiplicity (Kroupa 1995; Reid & Gizis 1997) lead to very

---

different luminosity functions at very low masses. The stellar multiplicity statistics also contains important information on both star formation processes and dynamical evolution of stellar systems, as reviewed for instance by Duquennoy & Mayor (1991).

While the binary statistics are now quite well determined for G (Duquennoy & Mayor 1991) and K dwarfs (Halbwachs et al. 1998), this is not yet the case for the fainter M dwarfs. The only well defined M-dwarf sample which has essentially complete multiplicity information is the (small) sample of M dwarfs within 5.2 pc (Henry & McCarthy 1990; Leinert et al. 1997). A number of programmes have searched for M-dwarf companions beyond this distance, using different techniques: radial-velocity monitoring (Bopp & Meredith 1986; Young et al. 1987; Upgren & Caruso 1988; Marcy & Benitz 1989; Tokovinin 1992; Upgren & Harlow 1996), deep infrared imaging (Skrutskie et al. 1989; Nakajima et al. 1994; Simons et al. 1996), astrometry and speckle or adaptive optics imaging (Henry & McCarthy 1992; Mariotti et al. 1992). Taken together, these programmes are however not sensitive to all binary separations for any statistically well defined sample. Reid & Gizis (1997) for instance compiled multiplicity information for a northern 8-pc sample, but had to conclude that, in spite of Henry & McCarthy's (1992) extensive speckle work, the information they could gather remained incomplete. The binary fraction derived from these data range from 26% (Leinert et al. 1997) to 42% (Fisher & Marcy 1992), through 33% (Reid & Gizis 1997). This seems to point towards a smaller fraction of multiple stars than the 57% found by Duquennoy & Mayor (1991) amongst G dwarfs, a result which would be an important input to multiple star formation theories. All of these estimates however suffer from either small number statistics or large incompleteness corrections, which are quite uncertain, as they sensitively depend on the (unknown) underlying multiplicity distribution.

Since September 1995, we have therefore been searching volume-limited samples of nearby M dwarfs for companions, combining three observing techniques which together ensure a good sensitivity at all separations for stars and brown dwarfs, and some useful sensitivity for giant planets:

- highly accurate ($10-70 \mathrm{~m~s}^{-1}$) radial velocities are measured with the ELODIE spectrograph at the Observatoire de Haute-Provence (Baranne et al. 1996), which was also used in the discovery of the first extra-solar planet (Mayor & Queloz 1995); they are combined with older CORAVEL data to extend our time base at lower accuracy;
- high angular resolution near infrared images are obtained with the ESO (ADONIS) and CFHT (PUE'O) adaptive optics systems, to directly detect relatively massive companions at small separations;
- deep adaptive optics coronographic infrared images (Beuzit et al. 1997) are obtained with ADONIS at ESO, since April 1997; they are sensitive to lower mass companions at slightly larger separations, and will be discussed in a forthcoming paper.

In this first paper, we present the radial-velocity programme, discuss its observing and data processing techniques in some detail, and present its first results together with some complementary adaptive optics data obtained with PUE'O. The observed sample and its completeness are discussed in Sect. 2 together with the observing strategy, while Sect. 3 discusses the radial-velocity and adaptive optics observations. Sect. 4 presents the results after 2.5 years, namely the discovery of 13 new M dwarfs and orbital elements for 7 of the new systems. Sect. 5 discusses the implications of the new systems for the solar neighbourhood population.

2. Sample selection and observing strategy

2.1. The sample

The observed radial-velocity sample is presented in detail by Delfosse et al. (1998b), who discuss the rotational properties of the same stars. Briefly, it contains all M dwarfs listed in the third edition of the nearby star catalogue (hereafter CNS3; preliminary version, Gliese & Jahreiss 1991) with a distance closer than 9 pc and a B1950.0 declination above $-16°$. 136 stars fulfill these criteria among which 7 have to be rejected because they are fainter than V=15 (the approximate sensitivity limit of the instrument we use), and another 2 because they are close companions to much brighter G dwarfs from which they cannot be separated by the spectrograph input fiber. At 9 pc the V=15 limit corresponds to an M6 dwarf, and at 5 pc to an M6.5 dwarf.

We have decided to observe a volume-limited sample because we are interested in a fair sampling of the local dwarf population, and want to derive unbiased statistical information. The quality of the distances listed in the CNS3 is however uneven, so this goal could only be partly reached. The new (4th) edition of the Yale General Catalogue of Stellar Trigonometric Parallaxes (Van Altena et al. 1995) and the HIPPARCOS catalogue (ESA 1997) together show that 11 sample stars are actually outside the nominal 9-pc sphere, while two omitted stars are actually within it. The 11 rejected stars have a disproportionately large fraction of nearly equal-mass multiple systems. Most of them were included in the initial sample on the basis of CNS3 photometric parallaxes. Their inclusion therefore largely reflects the $2^{3/2}$ volume bias incurred in using photometric parallaxes for unrecognized equal-mass binaries.

2.2. Observing strategy

Since no single observing technique is sensitive to companions over all separations, we have chosen to combine imaging and radial-velocity techniques, to maximize our sensitivity range.

As discussed below, the standard errors of the radial-velocity measurements range between 10 and $70 \mathrm{~m~s}^{-1}$, depending on apparent magnitude (and hence largely on spectral type, for this volume-limited sample). A $400 \mathrm{~m~s}^{-1}$ velocity amplitude is thus always easily detectable, even for the faintest stars. A $50 \mathrm{~m~s}^{-1}$ velocity amplitude is easily detectable for all stars brighter than approximately V=10. Fig. 1 shows how these conservative min-
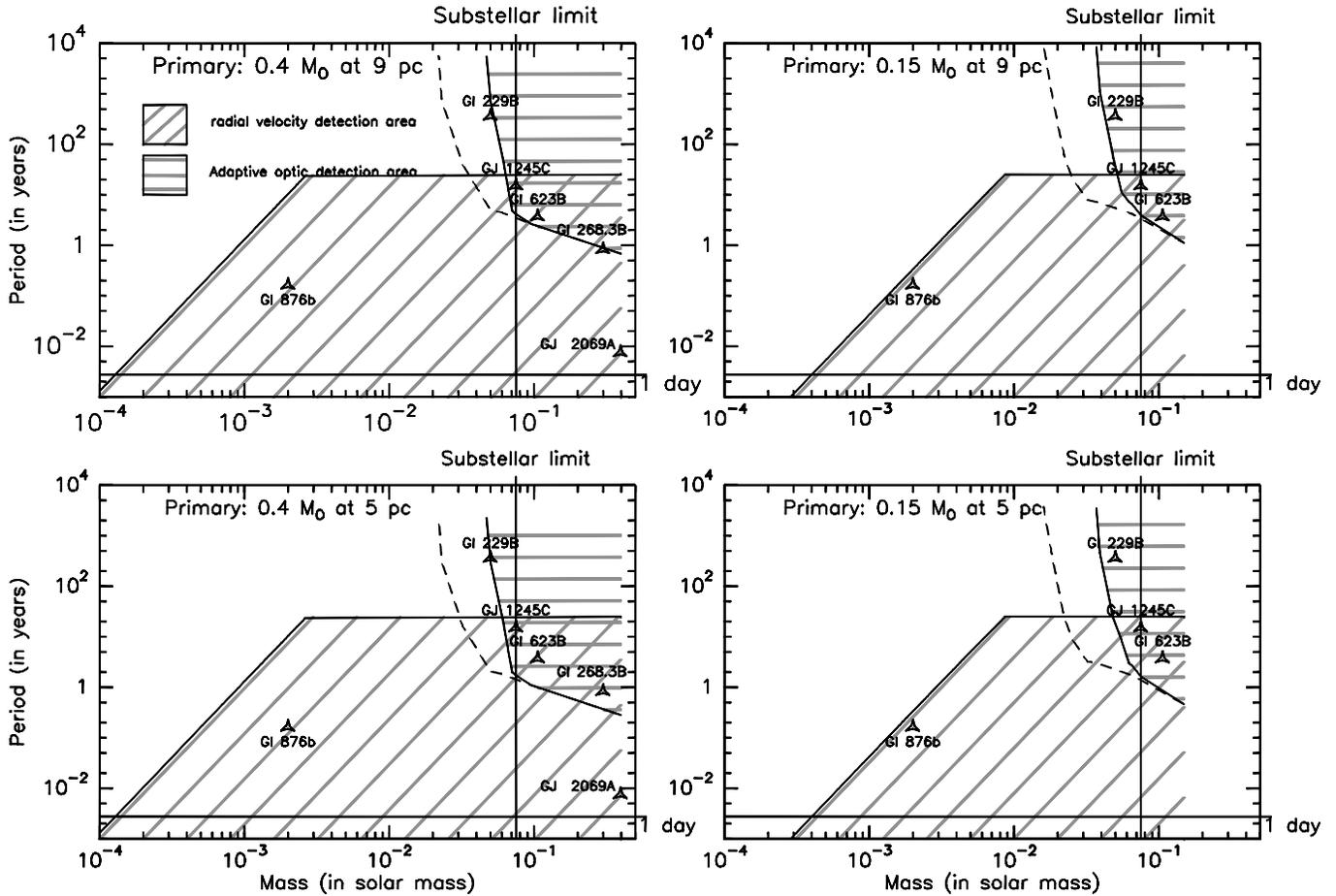
Fig. 1. Companion detectability in the $\log(P)$ versus $\log(M)$ plane for our radial-velocity and adaptive optics programmes. The 4 diagrams correspond to two representative primary masses of $0.4\,M_\odot$ ($\sim$ M2V, $M_K = 6.3$, Baraffe et al. 1998) and $0.15\,M_\odot$ ($\sim$ M5V, $M_K = 8.3$, Baraffe et al. 1998), at two representative distances of 5 and 9 pc. Typical radial-velocity accuracies are respectively 12 and 70 m s^{-1} for $0.4\,M_\odot$ and $0.15\,M_\odot$ stars. The radial-velocity detectability limits correspond to minimum amplitudes of 4σ, or respectively 50 and 300 m s^{-1}, and a maximum period of 25 years. Some longer period binaries will be detected, but the observing programme is unlikely to last long enough to determine their orbital elements. The solar metallicity models of the E.N.S Lyon group (Allard et al. 1996; Baraffe et al. 1998; Allard, Baraffe and Chabrier, private communication) for ages of 1 and 5 Gyr (dashed and solid lines, respectively) are used to transform the maximum detectable luminosity contrasts for PUE'O into approximate minimum companion masses. A few representative companions of M dwarfs have been added for illustration. Gl 623B and GJ 1245C are two of the least massive objects with dynamical mass determinations (Henry & McCarthy 1993). Gl 268.3B and GJ 2069Ab were discovered in the present programme. The brown dwarf Gl 229B (Nakajima et al. 1995) has a most probable mass of $0.05\,M_\odot$ (Allard et al. 1996). Gl 876b is the first planet discovered around an M dwarf (Delfosse et al. 1998d).

imum velocity amplitudes translate into minimum detectable companion masses as a function of orbital period, for two representative distances and primary masses, taking into account the better precision obtained with heavier (more luminous) primaries. For a one year orbital period, a 400 m s^{-1} velocity amplitude corresponds to a 5 Jupiter mass (M_J) body orbiting a $0.15\ M_\odot$ M4V-M5V primary, and 50 m s^{-1} corresponds to a $1.5\ M_J$ body orbiting a $0.4\ M_\odot$ M2V primary. Even though this programme was not chiefly devised to search for planets, it therefore has good sensitivity to them, as illustrated by our recent detection of a $\sim$2 M_J companion on a 2 month orbit around Gl 876 (Delfosse et al. 1998d; also Marcy et al. 1998). We will, a fortiori, be sensitive to all stellar and substellar companions with periods up to a few dozen years. The maximum period

at which we can actually detect stellar companions will be set by the duration of the observing programme rather than by the velocity amplitude (Fig. 1), as it is difficult to detect variability on timescales longer than about twice the time-span of the data. At 9 pc a limit of P$\sim$20 years translates into a minimum angular separation of $\sim$0.4″ for a 0.15 $M_\odot$ primary star and a companion of negligible mass (Fig. 1; this separation scales as $(M_1 + M_2)^{1/3}$).

The adaptive optics programme (hereafter AO) (Mariotti et al. 1992, Perrier et al. 1999) easily resolves equal-mass binaries down to separations as small as $0.08''$ (0.7 AU at 9 pc, corresponding to a $\sim$1 year period for an M-dwarf pair). It has a dynamic range in the K-band ($\lambda_0 = 2.2\ \mu$m) of 6.5 mag at a 0.25″ separation, 7.5 mag at 0.5″ and 8.5 mag at 1″. Since

the K-band absolute magnitudes of M0 and M8 dwarfs only differ by $\sim$5 mag (Leggett 1992), the AO observations can detect all main-sequence companions that the radial-velocity monitoring would miss (Fig. 1). For brown dwarfs on the other hand, we do have a small sensivity gap at intermediate separations: radial-velocity monitoring can for instance only detect a 0.05 $M_\odot$ Gl 229B-like brown dwarf orbiting a 0.4 $M_\odot$ M2V primary out to 5.4 AU (0.6″ at 9 pc), while AO imaging can only detect it beyond 1″. This gap disappears for later M-dwarf primaries or more nearby systems (Fig. 1), and the PUE'O adaptive optics system for instance easily detects Gl 229B itself, without a coronograph. Beyond 2″ (18 AU at 9 pc), the coronographic mode of the ESO adaptive optics system (Beuzit et al. 1997) can handle an extremely large contrast between the primary and a faint secondary ($\Delta m \sim$12.5 mag at 2″). We are thus again sensitive to all brown dwarf companions of M dwarfs, though not to planets.

Within the [0.4 AU, 4 AU] separation range (at 9 pc), the sensitivities of high precision radial velocities and adaptive optics overlap. In this range, the combination of the two techniques offers potential access to very accurate masses, as exemplified by Gl 570B (M1.5V+M3V) for which Forveille et al. (1999) obtain masses accurate to $\sim$2%. This should dramatically improve the mass-luminosity relation for the bottom of the main sequence.

3. Observations

3.1. ELODIE radial-velocity data

3.1.1. Instrumental setup

Most new radial-velocity observations were obtained at the Observatoire de Haute-Provence with the ELODIE spectrograph (Baranne et al. 1996) on the 1.93-m telescope, between September 1995 and May 1998. This fixed configuration dual-fiber-fed echelle spectrograph covers in a single exposure the 390–680 nm spectral range, at an average resolving power of 42000. An elaborate on-line processing is integrated with the spectrograph control software, and automatically produces optimally extracted and wavelength calibrated spectra, with algorithms described in Baranne et al. (1996). All stars in this programme are now observed with a thorium lamp illuminating the monitoring fiber, as needed for the best (~ 10 m s^{-1}) radial-velocity precision (Baranne et al. 1996). Before mid-1997 the fainter (V $\gtrsim$ 13 mag) stars were instead observed with this fiber illuminated by the sky, allowing subtraction of the diffused solar light whose lines could otherwise bias the velocity profile. The use of the new M4V correlation template (discussed below) has sufficiently reduced the sensitivity of the velocity measurements to sky emission that the standard high precision setup can now be used for all stars in this programme. These early data for faint stars have increased random zero-point errors, up to ~ 100 m s^{-1}.

A few measurements were also obtained with the CORALIE spectrograph on the newly commissioned 1.2-m Swiss telescope at La Silla Observatory (Chile). CORALIE is an improved copy of ELODIE and has very similar characteristics, with the exception of a substantially improved intrinsic stability and higher spectral resolution ($R = 50000$).

3.1.2. Data processing

The extracted spectra are analysed for velocity by digital cross-correlation with a one-bit (0/1) template. This processing is standard for ELODIE spectra (Queloz 1995a, 1995b), but the default K0III mask provided in the ELODIE reduction software is a relatively poor match to the much redder spectra of the programme stars. We have constructed a better adapted correlation template, applying the method of Baranne et al. (1979) to a high signal-to-noise (S/N=70) ELODIE spectrum of Gl 699 (Barnard's stars, M4V). The analysis was restricted to the [443 nm, 680 nm] spectral range, since bluer orders contain very little flux, for both Gl 699 and the programme stars. For each of the 48 ELODIE orders, 100 trial templates $g_0(\lambda)$ were generated by thresholding the rectified and normalized Gl 699 spectrum at 100 levels. We selected for each order the thresholding level which maximizes the quality factor defined by Baranne et al. (1979). The best order templates were then assembled into one global binary template, which has over 3100 "transparent" sections and a high overall transmission of 20.75%.

3.1.3. Measurement accuracy

For ELODIE, the radial-velocity precision can be written (Baranne et al. 1996, their Eq. (9)) as:

$$\varepsilon_p(V_r) = \frac{C(T_{eff})}{D\,S/N}\,\frac{(1+0.47\sigma)}{3}\,\mathrm{km\,s^{-1}}$$

where σ is the rotationally broadened 1/e half-width of the cross-correlation function (CCF), D its relative depth and S/N the signal-to-noise ratio in the reference 48$^{\mathrm{th}}$ ELODIE order. The $C(T_{eff})$ constant depends on both the correlation template used and the spectral type. Its values for the K0 and M4 templates were determined through Monte-Carlo simulations for the [M0V, M5.5V] spectral-type range. High signal-to-noise ratio spectra of 6 slowly rotating stars spanning the desired range of spectral type (selected from Delfosse et al. 1998b, Table 1) were degraded by synthetic photon and readout noise. The dispersion of the velocities measured from these spectra was then determined for a number of degraded signal-to-noise ratio values. The validity of the parameterization was verified on those synthetic data, and $C(T_{eff})$ was determined through a least square fit. It turned out to be constant over the M-dwarf spectral range. Its respective values for the K0 (Baranne et al. 1996) and M4 templates are 0.085 and 0.035 km s^{-1}. The radial-velocity standard errors for the two templates are presented in Fig. 2. The M4 template improves the accuracy by a factor of 2 at spectral type M0V, and by a factor of 10 at spectral type M4V. At a given signal-to-noise ratio, the accuracy variations as a function of spectral type mostly reflect changes in the relative depth of the CCF. The width of the CCF (Table 1) is essentially constant for the K0 template but significantly varies with spectral type for the M4 template. This change is small and does not appre-
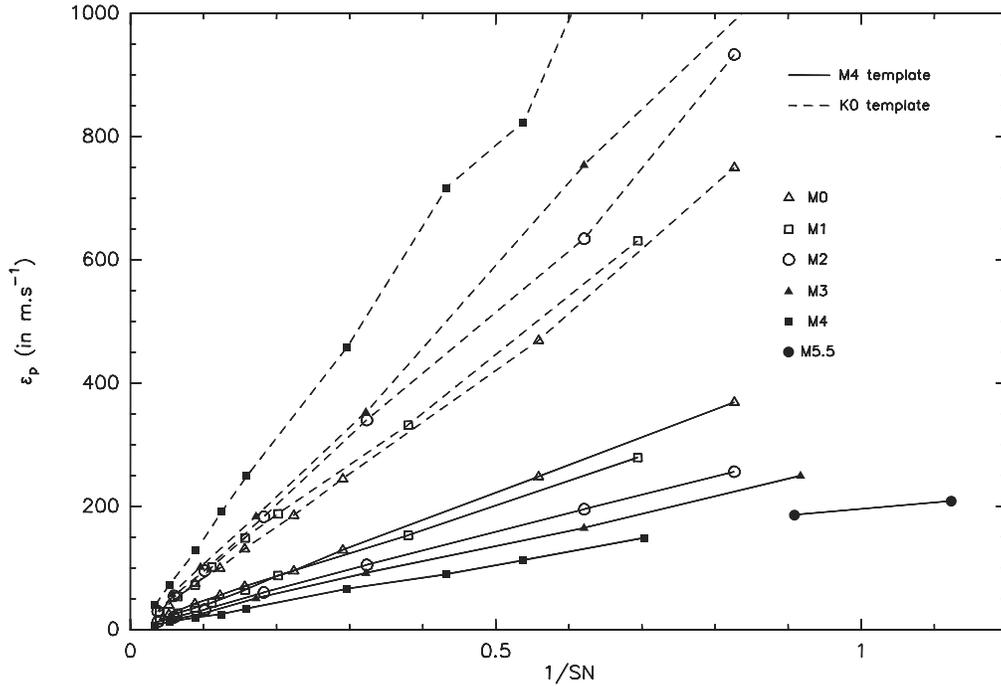
Fig. 2. Internal standard errors on radial velocity as a function of signal-to-noise ratio, for the two correlation templates (M4 and K0), and for stellar spectral types between M0 and M5.5.

Table 1. Width and depth of the CCF of 6 stars with spectral type in the [M0V,M5.5V] range, for the M4 and K0 templates. Spectral types are from Reid et al. (1995).

Spect. Type	$\sigma_{M4}(km\,s^{-1})$	D_{M4}	$\sigma_{K0}(km\,s^{-1})$	D_{K0}
M0 (Gl 424)	4.71	0.094	5.00	0.113
M1 (Gl 15A)	4.59	0.104	4.99	0.106
M2 (Gl 411)	4.39	0.119	4.94	0.096
M3 (Gl 725A)	4.32	0.140	4.87	0.082
M4 (Gl 699)	4.21	0.159	4.96	0.062
M5 (GJ 1002)	4.26	0.176		

ciably affect the precision of the radial-velocity measurements, but calibration of the CCF width in term of rotational velocity is substantially more difficult for the M4 template.

For the slowly rotating stars in our sample, the above formula predicts radial-velocity accuracies that range from $2\ \mathrm{m\,s^{-1}}$ for bright M0V (at typical S/N=200) to $70\ \mathrm{m\,s^{-1}}$ for faint M6V (at typical S/N=3). It is however clear that the lowest values are somewhat optimistic, as the (excellent) long term stability of ELODIE radial velocities is $\sim 12\ \mathrm{m\,s^{-1}}$ (Baranne et al. 1996). We have therefore quadratically added $12\ \mathrm{m\,s^{-1}}$ to the internal errors to account for instrumental stability. A fiber optics light scrambler was recently added to ELODIE to further stabilize the illumination of the spectrograph, and has improved the long term radial-velocity stability to below $10\ \mathrm{m\,s^{-1}}$. We have however chosen not to use this device, as its 20% light loss would degrade our overall measurement precision for stars fainter than V = 12.

Under some circumstances, the correction of the radial velocities to the solar system barycentre represents an additional limitation on the accuracy. At the latitude of Observatoire de Haute-Provence this correction can vary by up to $1.5\ \mathrm{m\,s^{-1}}$ per minute. It therefore significantly changes during the long exposure times (up to 1 hour) used for this programme, and it is important that the effective time of the observation be accurately determined. For bright stars a photomultiplicator monitors the fiber illumination of the spectrograph to compute its exact value. This P.M. is unfortunately too noisy to be used for our programme stars, and we have instead to use the mid-point of the observation. Under good atmospheric conditions this is not a problem, but when they are unstable (variable seeing or passing clouds) the two values can differ by up to a few minutes. In the worst case of unstable atmospheric conditions, a 1 hour exposure, and maximum variation of the barycentric correction, this additional error can reach $15\ \mathrm{m\,s^{-1}}$. It is usually much smaller.

Similar, but much larger, errors can affect measurements of very short period spectroscopic binaries (e.g. GJ 2069A, discussed below). Their velocities can vary by as much as $300\ \mathrm{m\,s^{-1}\,min^{-1}}$ (for P = 1 day), and even small errors on the effective time of the observation translate then into significant equivalent radial-velocity errors.

Magnetic activity is another important potential limitation for high-precision Doppler-velocity measurements of M dwarfs. Many of them have strong chromospheric activity, visible as H_α and Ca^+ H and K emission lines. The surface temperature of active stars is inhomogeneous, and since hotter parts are brighter, the velocity measured from the disk-integrated spectrum is biased towards the velocity of any hot spot, or away from the velocity of any cold spot. This effect is exacerbated when using a mismatched correlation template, such as the K0 template for M dwarfs: the K0 template is a better match to the hotter parts of the stellar surface and it therefore further increases their relative weight in the measured velocity.

On Julian day 2449978.5 (18.09.1995), a strong chromospheric flare in Gl 873 provides an extreme example of activity-

induced radial-velocity errors, and illustrates the much better immunity of the M4 correlation template. This generally active star presented on this date an activity well above its usual level. The H_α emission line showed a strong broad pedestal, characteristic (e.g. Jones et al. 1996) of active stars observed within about an hour of a major flare, and usually interpreted (Eason et al. 1992) as arising from mass motion of gas clumps with a large volume filling factor. With the K0 template, the radial velocity of Gl 873 for this date has a precision of $150 \, \mathrm{m\,s^{-1}}$ but differs from the median Gl 873 value by $1.7 \, \mathrm{km\,s^{-1}}$. With the M4 template on the other hand, the radial velocity precision for the same spectrum is improved to $15 \, \mathrm{m\,s^{-1}}$, and the measured value is within only $40 \, \mathrm{m\,s^{-1}}$ of the median velocity. Given the extreme character of the GL 873 event, $40 \, \mathrm{m\,s^{-1}}$ can thus be taken as an upper bound on the maximum radial-velocity error that can result from unusually high magnetic activity, when using the M4 mask.

The examination of the ~50 apparently single stars which have at least 3 good measurements (internal precision better than $20 \, \mathrm{m\,s^{-1}}$) shows that about half of them have apparent excess velocity dispersion at the $\sim 30 \, \mathrm{m\,s^{-1}}$ level. Gl 876 has been one of those until we very recently accumulated enough measurements to ascribe its velocity variability to a planetary companion (Delfosse et al. 1998d; also Marcy et al. 1998). Most of these stars however have few measurements, and it is thus not yet possible to determine how much of the apparent dispersion is due to intrinsic or instrumental radial-velocity noise, and how much is due to yet unrecognized companions, either planetary ones in short-period orbits or more massive distant ones. The exact accuracy limits of this programme are thus still undetermined, but are better than $\sim 30 \, \mathrm{m\,s^{-1}}$.

Double-lined spectroscopic binaries are in addition affected by a phase-dependent systematic error source. The Gaussian profile adjustment which is used to measure the radial velocity only imperfectly describes the correlation profile of an M dwarf, whose baseline shows some low level (~1%) systematic undulations. For a single star, or a single-lined binary, this has no effect on the measured velocity, or perhaps introduces a small constant zero-point offset. For double-lined binaries on the other hand, the correlation peak of one star is superposed onto a systematically different part of the other star's baseline, producing phase-dependent velocity errors. If the velocity amplitudes are of the order of the width of the the two correlation profiles, these are systematic errors and they will bias the derived orbital elements, and in particular the amplitudes. When the amplitudes are sufficiently larger than the width of the profiles on the other hand, these velocity errors become random, and the orbital elements then only have increased uncertainties but are unbiased. Under the same circumstances, and with enough measurements, it is also possible to separately determine the correlation profiles of the two components, and to correct the velocities for the effect of their baseline wiggles, for instance with the iterative method used by Forveille et al. (1999) for Gl 570B. For smaller velocity amplitudes this method cannot be used, and one would have instead to rely on the correlation profile of a matched spectral template, introducing some additional uncer-

tainties. We haven't yet applied any such correction except to Gl 570B, and SB2 velocities thus have errors of $\sim 100 \, \mathrm{m\,s^{-1}}$ or larger (for the fainter component in particular).

3.2. CORAVEL radial-velocity data

65 bright ($V \lesssim 12$) stars in the sample had previously been measured in the course of various observing programmes using the older CORAVEL spectrographs (Baranne et al. 1979) on the 1-m Swiss telescope (at Observatoire de Haute-Provence, France) and the 1.54-m Danish telescope (La Silla Observatory, ESO, Chile). The number of measurements varies considerably, from 2–3 for stars examined in the course of the HIPPARCOS follow-up survey (Udry et al. 1997), to over 100 for a few well studied previously known binaries. They have lower precision than the ELODIE measurements (at best $300 \, \mathrm{m\,s^{-1}}$, and often 1–$2 \, \mathrm{km\,s^{-1}}$ for the present faint red stars), but, when available, they extend the time base to typically 10 years. These data are thus systematically extracted from the CORAVEL database for all programme stars. There is a significant radial velocity offset between CORAVEL and ELODIE measurements (Udry et al. 1998), which must be corrected before they can be combined. For G-K dwarfs the offset depends upon both spectral type and radial velocity. Over the [M0V, M3.5] range where we have common measurements the offset is independent of spectral type, but has a significant uncalibrated star to star scatter at the $\sim 600 \, \mathrm{m\,s^{-1}}$ level. For well observed binary stars, the CORAVEL offset is thus determined as part of the orbital element adjustment.

3.3. Adaptive optics data

3.3.1. Instrumental setup

The observations were carried out at the 3.6-meter Canada-France-Hawaii Telescope (CFHT) during several observing runs from September 1996 to March 1998, using the CFHT Adaptive Optics Bonnette (AOB) and two different infrared cameras. The AOB, also called PUE'O, is a general purpose adaptive optics (AO) system. It is mounted at the F/8 Cassegrain focus, and cameras and other instruments are then attached to it (Arsenault et al. 1994, Rigaut et al. 1998). It analyses the atmospheric turbulence with a 19 element wavefront curvature sensor and corrects for it with a 19 degree of freedom bimorph mirror. Modal control and continuous mode gain optimization (Gendron and Léna 1994; Rigaut et al. 1994) maximize the correction quality for current atmospheric turbulence and guide star magnitude. For our observations a dichroic mirror diverted the visible light to the wavefront sensor while a science detector recorded near-infrared light. The data were recorded with either MONICA, the Université de Montréal Infrared Camera (Nadeau et al. 1994), or KIR, a new CFHT infrared camera developed to take full advantage of the AO corrected images produced by PUE'O (Doyon et al. 1998).

MONICA was used for the commissioning of the AOB during the first semester 1996 and for all science runs until Novem-

Table 2. New low mass companions in the solar neighbourhood (the companion of Gl 876 is a planet). Spectral types are from Reid et al. (1995), except for GJ 2130B which is taken from the CNS3 catalogue. Parallaxes (in milliarcseconds) are taken from (a) the HIPPARCOS catalogue, (b) the Yale catalogue (Van Altena et al. 1995) or (c) are photometric parallaxes from the CNS3.

Name	parallax (mas)	joint spectral type
LP 476–207 AabB	$91.20 \pm 8.56^{(a)}$	M 4
Gl 268.3 AB	$81.05 \pm 2.42^{(a)}$	M 2.5
GJ 2069 Aab	$78.05 \pm 5.69^{(a)}$	M 3.5
GJ 2069 BC	$78.05 \pm 5.69^{(a)}$	M 4
LHS 6158 AabB	$224.0 \pm 36.0^{(c)}$	M 3.5
Gl 381 AB	$81.23 \pm 2.37^{(a)}$	M 2.5
Gl 487 AabB	$98.14 \pm 1.67^{(a)}$	M 3
LHS 2887 AB	$62.2 \pm 13.1^{(b)}$	M 4
G 203–047 ab	$137.84 \pm 8.95^{(a)}$	M 3.5
GJ 2130 Bab	$161.77 \pm 11.29^{(a)}$	M 2.5
Gl 829 ab	$148.29 \pm 1.85^{(a)}$	M 3.5
Gl 876 ab	$212.69 \pm 2.10^{(a)}$	M 4
Gl 896 Aab	$160.06 \pm 2.81^{(a)}$	M 3.5
Gl 896 Bab	$160.06 \pm 2.81^{(a)}$	M 4.5

ber 1997. It is a facility instrument based on a NICMOS3 256 × 256 detector, and was originally designed by the Université de Montréal for the Observatoire du Mont Mégantic and CFHT F/8 Cassegrain focii. The camera was refitted with new optics for use at the F/20 output focus of AOB. It produces a plate scale of 0.″034 per pixel, properly sampling diffraction-limited images down to the J band (1.25 μm). The resulting field size is 8.7″ × 8.7″.

Since December 1997, MONICA has been replaced on PUE'O by KIR, a new imaging camera which records a 16 time larger field on an HAWAII 1024 × 1024 HgCdTe array. KIR has improved optical quality and detector read-out noise, and therefore a significantly better detectivity. The KIR plate scale is 0.″035 per pixel, for a total field size of 36″ × 36″.

3.3.2. Observations

Sources were first examined for binarity with one filter, usually H (1.65 μm). Under good to moderate seeing conditions H represents the best compromise between sensitivity, corrected image quality, and sky brightness. Under worse seeing conditions the K filter was used instead to maintain acceptable image quality. Sources which saturate the detectors in the minimum available integration time through the H (1.65 μm) or K(2.23 μm) broad-band filter (brighter than K = 7 under typical conditions) were observed through corresponding narrow-band filters, respectively [Fe$^+$] (1.65 μm) and H$_2$ (2.12 μm). Whenever a target appeared double, it was further observed with additional filters to determine relative colour indices. Integration times per frame typically range between a few tenths of a second and a few seconds. In order to improve the signal-to-noise ratio and to

average the residual uncorrected atmospheric turbulence, series of ∼4 minute total integration times were accumulated in a four position mosaic pattern. This observing sequence also allows to correctly determine the sky background and to correct for detector cosmetic defects. Wavefront sensing was performed on the sources themselves, which are always bright enough (R < 14) to ensure diffraction-limited images in H and K bands under standard Mauna Kea atmospheric conditions (i.e. seeing up to 1″). For most targets, PSF calibration stars were observed under the same conditions to provide input to parameter fitting (Sect. 3.3.3) and image deconvolution. The atmospheric turbulence and AO correction for a given set of observations were further characterized by simultaneously recording the wavefront sensor measurements and deformable mirror commands. An accurate synthetic PSF can be generated a posteriori from these ancillary data, as described by Véran et al. (1997). Astrometric calibration fields such as the central region of the Trapezium Cluster in the Orion Nebula (McCaughrean and Stauffer 1994), were observed to accurately determine the actual detector plate scale and position angle (P.A.) origin. Flat-fields were obtained on the dome and the sky for each filter.

3.3.3. Data reduction

For each filter, the raw images were median combined to produce sky frames which were then subtracted from the raw data. Subsequent reduction steps included flat-fielding, correction from the bad pixels, and finally shift-and-add combinations of the corrected frames into a final image. For resolved binary systems, the separation, position angle and magnitude difference between the two stars were determined using *uv* plane model fitting in the GILDAS (Grenoble Image and Line Data Analysis System) software. With approximate initial values of the positions of the two components along with a PSF reference image, the fitting procedures gave as output the flux and pixel coordinates of the primary and secondary. Application of the astrometric calibrations then yields the desired parameters. Images of the newly resolved binaries are presented in Fig. 4.

4. New companions

In this section we comment the new companions individually. A general view of their measurements (visual and spectroscopic) and status (new discovery, first orbit determination, etc.) is summarized in Table 3. If determined the orbital elements are given in Table 4 and some interesting visual parameters in Table 5.

4.1. LP 476–207 AabB

LP 476–207 is a new triple system. Adaptive optics images show a 0.97″ separation pair with a K-band magnitude difference of 0.9 (Table 5), confirming a recent speckle detection of this outer component by Henry et al. (1997). The brightest component of the visual pair, LP 476–207 A, is a new large amplitude double-lined spectroscopic binary, with a period of P∼12 days. The visual pair was also detected by HIPPARCOS (ESA 1997),
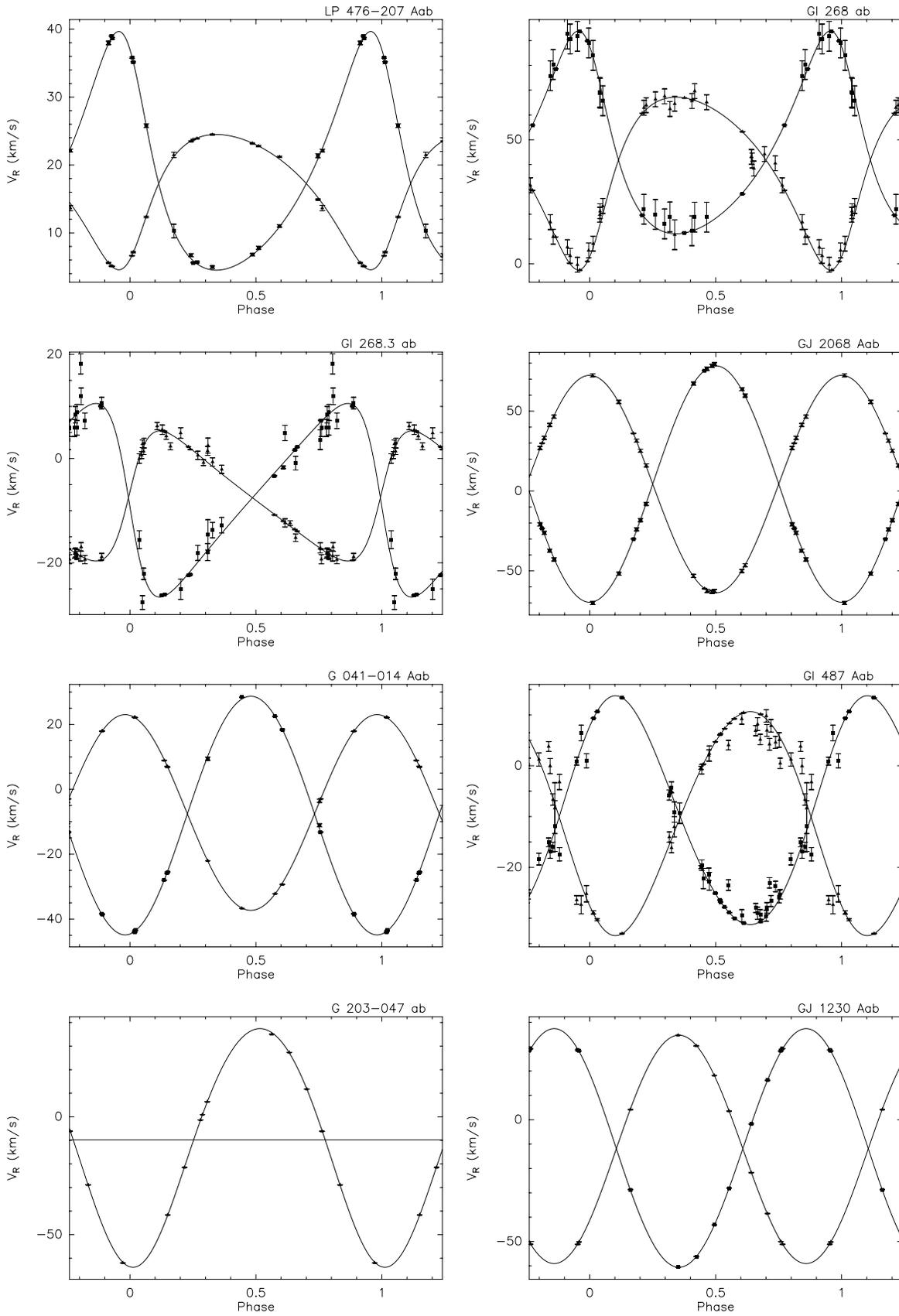
Fig. 3. Radial-velocity orbits. Triangles correspond to radial velocities of the primary star and squares to those of the secondary star.
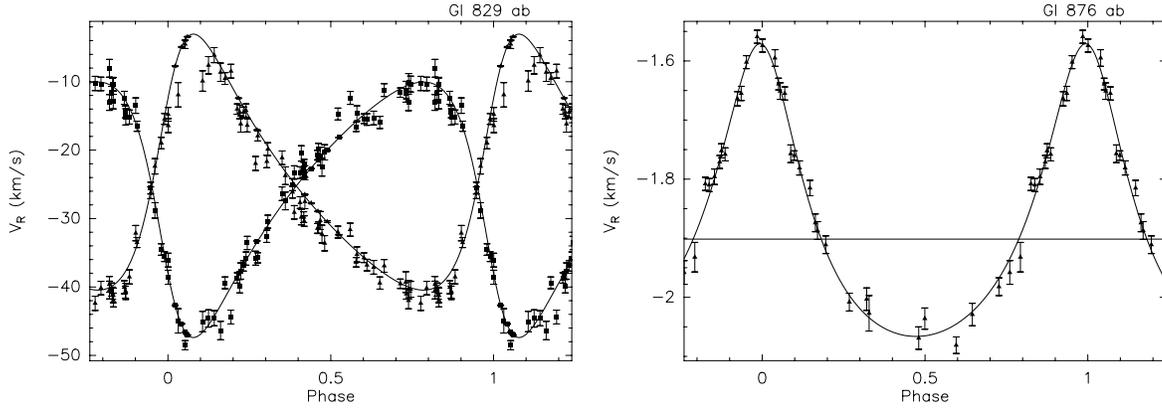
Fig. 3. (continued)

Table 3. Measurement summary: COR, ELO and PUE'O are the number of measurements obtained with CORAVEL, ELODIE and PUE'O, respectively. Gl 644 and Gl 866 are not included here, since their discussion is deferred to a forthcoming paper (Delfosse et al. in preparation). To date (September 1998), this programme has identified 13 new stellar companions and 1 planet orbiting M dwarfs of the solar neighbourhood. Orbital elements have been determined for six of them, as well as for 3 previously known binaries with undetermined orbits (LHS 6158 Aab and G 203–047 ab, Reid & Gizis (1997); GJ 1230 Aab, Gizis & Reid (1996)).

Name	COR	ELO	PUE'O	discovered by this programme	first orbit determination	orbit improvement	In the 9-pc sample
LP 476-207 Aab	0	16	3	yes	yes	–	no
LP 476-207 AB	0	16	3	no	no	no	no
Gl 268 ab	0	9	1	no	no	yes	yes
Gl 268.3 AB	29	10	3	yes	yes	–	no
GJ 2069 Aab	0	18	1	yes	yes	–	no
GJ 2069 BC	0	5	1	yes	no	no	no
LHS 6158 Aab	0	14	2	no	yes	–	yes
LHS 6158 AB	0	14	2	yes	no	no	yes
Gl 381 AB	27	4	2	yes	no	no	no
Gl 487 Aab	24	18	5	yes	yes	–	no
Gl 487 AB	24	18	5	yes	no	no	no
LHS 2887 AB	0	5	2	yes	no	no	no
G 203-047 ab	0	12	1	no	yes	–	yes
GJ 2130 Bab	0	1	0	yes	no	no	yes
GJ 1230 Aab	0	11	0	no	yes	–	yes
Gl 829 ab	67	11	1	yes	yes	–	yes
Gl 876 ab	0	32	1	yes	yes	–	yes
Gl 896 Aab	0	9	1	yes	no	–	yes
GL 896 Bab	0	6	1	yes	no	–	yes

which lists a separation of 0.68″. There has thus been significant orbital motion over the last ∼5 years.

4.2. Gl 268 ab

Gl 268 is a previously known double-lined binary on a 10.43-day orbit (Tomkin & Pettersen 1986). Our new spectroscopic measurements provide substantially improved orbital elements.

4.3. Gl 268.3 AB

Gl 268.3 is a new double-lined spectroscopic binary. With respectively 29 and 10 CORAVEL and ELODIE measurements,

spanning over 15 years, the radial-velocity orbit is extremely well determined. The period is 304.35±0.25 days. K-band adaptive optics images partly resolve this system into a ∼0.1″ binary with a small magnitude difference (Table 5). Within one or two years Gl 268.3 will thus provide two precise mass determinations at a spectral type of M2.5V.

4.4. GJ 2069 AabBC

Previously known as a wide (∼ 12″) visual binary, the GJ 2069 system is actually quadruple. Adaptive optics images resolve GJ 2069B into a 0.36″ binary with a K-band magnitude difference of 0.45 (Table 5). The 5 radial-velocity measurements

Table 4. Orbital elements and M sin$i$ for the newly determined radial-velocity orbits. The inclination of GJ 2069 Aab is accurately known and we thus list the actual masses instead of M sin$i$. G203–47 and Gl 876 are single-lined binaries (all others are double-lined), so we list $f_1(M)$ as well as estimated M$_2$ sin$^3 i$ for assumed primary masses of, respectively, 0.35 and 0.30 M$_\odot$.

Name	P (days)	T_0 (Julian day)	e	ω	K_1 (km s^{-1})	K_2 (km s^{-1})	V_0 (km s^{-1})	mass determination (M$_\odot$)	
Double-lined binaries: M$_1 \times$ sin i and M$_2 \times$ sin i								M$_1$ sin$^3 i$	M$_2$ sin$^3 i$
LP 476-207 Aab	11.9623 ±.0005	49799.47 ±0.04	0.323 ±.006	212.0 ±0.6	9.96 ±0.03	17.57 ±0.07	17.26 ±0.03	0.014 ±.0001	0.008 ±0.0001
Gl 268 ab	10.4265 ±.00002	50149.902 ±0.008	0.321 ±.001	212.1 ±0.3	34.81 ±0.04	40.86 ±0.06	41.83 ±0.03	0.215 ±.001	.183 ±.001
Gl 268.3 AB	304.35 ±.25	48826.0 ±1.5	0.399 ±.008	273.8 ±0.9	12.47 ±0.08	18.6 ±0.2	-7.51 ±0.05	0.435 ±.010	0.292 ±.006
LHS 6158 Aab	7.5555 ±.0002	50471.2 ±0.2	0.014 ±.002	7.0 ±9.3	30.15 ±0.05	36.79 ±0.09	-7.57 ±0.04	0.129 ±.001	.106 ±.001
Gl 487 Aab	54.075 ±.006	50506.2 ±0.5	0.081 ±.005	137.0 ±3.0	22.0 ±0.5	22.5 ±0.5	-10.1 ±0.4	0.247 ±.014	0.242 ±.013
GJ 1230 Aab	5.06880 ±.00005	50643.7 ±0.2	0.009 ±.001	230.0 ±10.0	46.9 ±0.1	49.0 ±0.1	-11.88 ±0.05	0.237 ±.001	0.226 ±.001
Gl 829 ab	53.221 ±.004	48980.2 ±0.2	0.374 ±.004	300.0 ±1.0	18.7 ±0.1	18.7 ±0.1	-25.23 ±0.06	0.114 ±.001	0.114 ±.001
Single-lined binaries: $f_1(M)$ and an estimate of M$_2$ sin$^3 i$								$f_1(M)$	M$_2$ sin$^3 i$
G203-47 Aab	14.7136 ±.0005	50500.8 ±0.1	0.068 ±.004	175.0 ±3.0	50.6 ±0.2	– –	-9.7 ±.2	0.2 –	$\sim$0.5 –
Gl 876 ab	61.1 ±.2	50661.7 ±1.5	0.33 ±.02	5.0 ±5.0	0.247 ±0.006	– –	-1.901 ±0.005	8.10^8 –	$\sim$0.002 –
Double-lined eclipsing binary: complete determination of M$_1$ and M$_2$								M$_1$	M$_2$
GJ 2069 Aab	2.771472 ±.000004	50207.8128 ±0.0009	0.0 ±.003	– –	68.03 ±0.09	73.06 ±0.09	4.36 ±0.04	0.430 ±.001	0.396 ±.001

Table 5. Projected separation and luminosity contrast at K band, for binaries resolved by adaptive optic imaging.

Name	Separation	ΔK (mag)	Observing date
LP 476-207 AB	0.97″±0.01″	0.9±0.05	Jan 1997
Gl 268.3 AB	marginally resolved $\sim$0.1″		May 1997
GJ 2069 BC	0.36″±0.01″	0.45±0.3	May 1997
LHS 6158 AB	0.62″±0.01″	0.50±0.04	Jan 1997
Gl 381 AB	0.18″±0.02″	0.95±0.05	Aug 1997
Gl 487 AB	0.23″±0.01″	0.7±0.1	Feb 1997
LHS 2887 AB	0.58″±0.01″	0.15±0.03	May 1997

obtained over $\sim$850 days show a linear drift of $\sim 600 \mathrm{~m\,s}^{-1}$. The period is thus probably long and the small visual separation may be due to projection.

GJ 2069A is a new short-period (P = 2.8 days) detached double-lined eclipsing binary, only the third one known with substantially sub-solar masses. Delfosse et al. (1998c) discuss in detail the very accurate radial-velocity orbit and a preliminary light curve. They derive individual masses (0.430 and 0.396

M$_\odot$) with 0.4% accuracy. Both components are clearly sub-luminous for their masses, and their spectral types are later than expected, compared with both solar metallicity stellar models and previous stellar mass determinations. This indicates a metal-rich composition.

4.5. LHS 6158 (G 041–014) AabB

Recently shown to be a short-period double-line spectroscopic binary (Reid & Gizis 1997), G 41–14 is actually a triple system. We have determined the orbital elements ($P = 7.6$ days) of the close spectroscopic pair, and discovered a third component in AO images, at a separation of 0.62″ and with a K-band magnitude difference of 0.5 (Table 5). The probable period is $\sim$10 years and a mass determination is thus a mid-term prospect only.

4.6. Gl 381 AB

This new long-period double-line spectroscopic binary is also well resolved into a 0.18″ pair (ΔK=0.95 mag) in AO images (Table 5). The period is relatively well determined at $\sim$2845 days, but the CORAVEL measurements do not sepa-
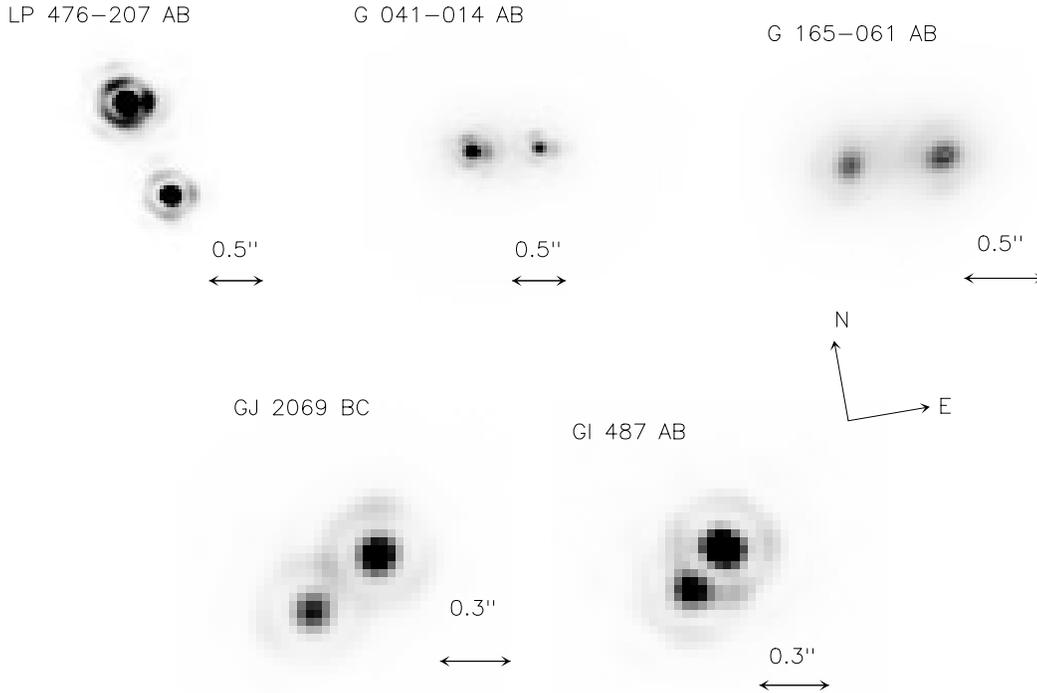
Fig. 4. Adaptive optics images for 5 of the new binaries.

rate the two components well and the ELODIE data only cover a small fraction of the orbit. All other orbital elements are thus still uncertain. ELODIE will easily separate the two stars at periastron. This spectroscopic + visual pair will then provide accurate mass measurements, within about 5 years.

4.7. Gl 487 AabB

Gl 487 is a new triple-line spectroscopic system. The short period (for Gl 487Aab) is 54.07 days and the long period is approximately 3000 days. The outer system (Gl 487 AB) is also resolved in AO images with a separation of $0.23''$ and $\Delta K=0.7$ mag (Table 5). This system has the potential to provide three accurate mass determinations, but its complete analysis is deferred to a forthcoming paper (Delfosse et al. in preparation) dealing with triple systems.

4.8. LHS 2887 (G165–061) AB

The probable period of this new double-line spectroscopic binary is a few years (1500 days for a very preliminary orbit). It is also well resolved in AO images, with a separation of $0.58''$ (Table 5) and will eventually provide accurate masses.

4.9. Gl 644

Our spectroscopic measurements confirm that the speckle binary Gl 644 (Tokovinin & Ismailov 1988) is a triple system, as previously shown by Eggen (1978) and Pettersen et al. (1984). We have decoupled the two orbits, and obtained preliminary values for the masses of the three stars. Their accuracy would however benefit from additional measurements and their dis-

cussion is thus deferred to a forthcoming paper (Delfosse et al., in preparation).

4.10. G 203–047 ab

This M3.5V star was previously noted as a single-line spectroscopic binary by Reid & Gizis (1997). We have obtained orbital elements, with a 15-day period, a large velocity semi-amplitude of $50\ \mathrm{km\,s^{-1}}$, and a small and only marginally significant eccentricity of 0.07. It is listed in the HIPPARCOS catalogue as a probable short-period astrometric binary without orbital solution. Now knowing the period, it would be of interest to reanalyse the HIPPARCOS data, and extract the inclination. The orbital elements result in a large mass function, $(M_2\ \sin i)^3/(M_1 + M_2)^2\ =\ 0.2\,\mathrm{M_\odot}$, and therefore imply a quite massive secondary. Adopting the Baraffe et al. (1998) theoretical mass-luminosity relation, the mass of the M3.5V primary (M_I=8.87, Figueras et al. 1990) is 0.30-0.35 $\mathrm{M_\odot}$, and the measured mass function thus requires that the secondary component be more massive than $\sim 0.5\,\mathrm{M_\odot}$. This clearly excludes a single-main sequence star, which would have a spectral type earlier than M1V and would dominate the observed light. A (very) short-period main-sequence binary is similarly excluded, because its brighter member would still need to be at least about as massive as the primary, and would be easily visible in the spectrum. The companion to G 203-047 must thus be a degenerate star. It is most likely a white dwarf, since visible photometry of G 203-47 (Figueras et al. 1990) shows a $\sim$0.4 U-B excess over the colour of stars with the same R-I colour or spectral type (Leggett 1992). UV spectroscopy would easily ascertain the exact characteristics of the white dwarf. The small semi-major axis of the present orbit ($a_1 \sin i\ =\ 14.5\,\mathrm{R_\odot}$, or 0.05 AU) implies that G 203-47a must have been, at previous

stages, in a contact configuration with the AGB progenitor of its white dwarf companion. It is therefore a very nearby member of the pre-cataclysmic variable family (e.g. Ritter & Kolb 1998), but the timescales for its evolution into a CV is extremely long. It should have accreted some nucleosynthesis products dredged up to the surface of its previous AGB companion, and its composition may thus be peculiar.

4.11. GJ 2130 ABab

At $\delta = -32°$, the little studied GJ 2130 system is far below the declination limit of the main sample and was observed as part of a possible southern extension of the programme. GJ 2130B, the fainter component of this wide (25″ separation) visual binary turns out to be a double-lined spectroscopic binary, and the system is thus triple. To date we don't have enough radial-velocity data to attempt an orbital solution.

4.12. GJ 1230 AabB

GJ 1230A, the brighter component of the wide (5″ separation) GJ 1230AB visual binary is a double-lined spectroscopic binary (Gizis & Reid 1996), for which we determine first orbital elements. The period is 5.1 days.

4.13. Gl 829 ab

Gl 829 was mentioned as a possible double-lined spectroscopic binary by Marcy et al. (1987). It is clearly seen as such by both CORAVEL (67 measurements) and ELODIE (11 measurements) and the orbital elements are well constrained. The orbital period is 53.2 days and the mass ratio is very close to 1.

4.14. Gl 866

We confirm that the astrometric and speckle binary Gl 866 (Leinert et al. 1986) is a triple system, as long suspected from the mass excess of one of the speckle components (Leinert et al. 1990). It is seen as a triple-lined spectroscopic system in the ELODIE spectra. The extensive speckle coverage of its outer orbit (Leinert et al. 1990) makes it a prime candidate for an accurate mass determination. As for Gl 644, the two decoupled orbits and the resulting masses will be discussed in a forthcoming paper (Delfosse et al., in preparation).

4.15. Gl 876 ab

High precision radial-velocity observations of the nearby M4 dwarf Gl 876 with the Observatoire de Haute-Provence 1.93-m telescope and the new 1.20-m Swiss telescope at La Silla indicate the presence of a Jovian mass companion to this star. The orbital fit to the data gives a period of 60.96 days, a velocity amplitude of 248 m s^{-1} and an eccentricity of 0.34. Assuming that Gl 876 has a mass of 0.3 M$_\odot$, the mass function implies a mass for the companion of $2/\sin i$ Jupiter masses. Delfosse et

al. (1998d) and Marcy et al. (1998) both discuss this interesting system in detail.

4.16. Gl 896 AabBab

The Gl 896 system, well known as a wide binary, is actually quadruple: both members of the visual pair are new single-lined spectroscopic binaries. Their probable periods are of the order of a few years but still undetermined. We have observed both of them with adaptive optics in December 1997 and not resolved either. The luminosity contrast of the companions is thus probably large.

5. Discussion

After 2.5 years, we have found 12 new companions to the 127 M dwarfs in our initial sample, and over the same period 6 additional companions were discovered by others (we also independently found most of those). While showing that the multiplicity information was previously fairly incomplete, this should not be taken as the final number of companions for this sample. Many stars still have few radial-velocity measurements (the median is 5 but a number of stars only have 2 measurements), which span an interval of at most 2.5 years. Our detectivity is thus very significantly biased towards nearly equal-mass binaries (detectable as double-lined binaries in a single measurement) or/and short periods. A significant number of lower mass companions in wider orbits certainly remains to be found in this sample.

The discovery of this large number of new multiple systems has two opposite effects on estimates of the stellar density in the solar neighbourhood. On the one hand, the new components within 9 pc increase the previously underestimated local density, typically with lower mass stars as they are necessarily fainter than their primaries. On the other hand, a number of previously unknown M-dwarf binaries are actually beyond the 9-pc distance limit of the sample, in which they were initially included on the basis of an underestimated photometric distance, reflecting the well known $\sim 2^{3/2}$ volume bias in photometric parallaxes of unrecognized binaries. This second correction decreases the local density, more or less uniformly for all masses. These two effects have been abundantly discussed in the context of photometric luminosity functions, as a possible explanation of their differences from the solar neighborhood luminosity function (e.g. Kroupa 1995, and Reid & Gizis 1997, for two contrasted views). It is perhaps not always recognized that, beyond ~ 5 pc, the solar neighborhood luminosity function still has a significant photometric component, and that it is thus also affected at some level by the same two effects.

Taking together newly published trigonometric parallaxes (ESA, 1997; Van Altena at al. 1995) and corrected photometric distances to the new binaries, 13-M-dwarf systems listed within 9 pc in the preliminary version of the CNS3 are actually beyond this distance, while only one system (Gl 203) enters this volume. The better observed 5.2-pc sample, on the other hand, is essentially unaffected, with only the G041-014 system removed (~ 4.5 pc $\rightarrow$ ~ 8 pc) from it. The previously mentioned (e.g.

Henry et al. 1994) incompleteness of the nearby M-dwarf system sample beyond 5 pc is thus made more significant. Systems with bright secondaries are rapidly recognized as double-lined binaries, and their inventory should thus be essentially complete. The remaining 7 photometric parallaxes in this revised 9-pc sample can therefore be considered as reliable. The 9-pc northern sample of systems should thus now only significantly change through inclusion of presently missing systems.

The new multiple systems, on the other hand, add 6 stars to the 9-pc sample of stars. Given the remaining selection biases in our binary search, we feel that derivations of the binarity statistics and stellar luminosity function within 9 pc would still be premature.

Our sensitivity to lower companion masses and longer periods is however quickly improving, so that this information will soon become available. It will then be possible to more reliably estimate the correction for unresolved binaries in photometric determinations of the luminosity function, and hopefully settle the long-standing controversy (e.g. Kroupa 1995 and Reid & Gizis 1997) on its true importance.

References

Allard F., Hauschildt P.H., Baraffe I., Chabrier I., 1996, ApJ 465, 123

Arsenault R., Salmon D., Kerr J., et al., 1994, In: Ealey M.A., Merkle F. (eds.) SPIEE Proceedings 2201, Adaptive Optics in Astronomy. 833

Baraffe I., Chabrier G., Allard F., Hauschildt P.H., 1998, A&A 337, 403

Baranne A., Mayor M., Poncet J.L., 1979, Vistas in Astronomy 23, 279

Baranne A., Queloz D., Mayor M., et al., 1996, A&AS 119, 373

Beuzit J.L., Mouillet D., Lagrange A.M., Paufique J., 1997, A&A 125, 175

Bopp B. W., Meredith R., 1986, PASP 98, 772

Delfosse X., Tinney C.G., Forveille T., et al., 1997, A&A 327, L25

Delfosse X., Tinney C.G., Forveille T., et al., 1998a, A&AS, in press

Delfosse X., Forveille T., Perrier C., Mayor M., 1998b, A&A 331, 581

Delfosse X., Forveille T., Mayor M., Burnet M., Perrier C., 1998c, A&A letter, submitted

Delfosse X., Forveille T., Mayor M., et al., 1998d, A&A 338, L67

Doyon R., Nadeau D., Vallee P., et al., 1998, In: Fowler A.M. (ed.) SPIE Proceedings 3354, Infrared Astronomical Instrumentation

Duquennoy A., Mayor M., 1991, A&A 248, 485

Eason E., Giampapa M., Radick R., Worden S., Hege E., 1992, AJ 104, 1161

Eggen O.J., 1978, ApJ 226, 405

ESA, 1997, The HIPPARCOS Catalogue. ESA SP-1200

Figueras F., Jordi C., Rossello G., Torra J., 1990, A&ASS 82, 57

Fischer D.F., Marcy G.W., 1992, ApJ 396, 178

Forveille T., Beuzit J.L., Perrier C., et al., 1999, A&A, in preparation

Gendron E., Léna P., 1994, A&A 291, 337

Gizis J.E., Reid I.N., 1996, AJ 111, 365

Gliese W., Jahreiss H., 1991, Preliminary Version of the Third Catalogue of Nearby Stars, as available at CDS Strasbourg

Halbwachs J.L., Mayor M., Udry S., 1998, In: Rebolo, Martin, Zapaterio-Osorio (eds.) Brown Dwarfs & Extra-solar Planets. ASP conf. series. vol. 134, p. 308

Henry T.J., McCarthy Jr D.W., 1990, ApJ 350, 334

Henry T.J., McCarthy Jr D.W., 1992, In: McAllister, Hartkopf (eds.) (ASP) Complementary Approaches to Double and Multiple Stars Research. p. 10

Henry T.J., McCarthy Jr D.W., 1993, AJ 106, 773

Henry T.J., Kirkpatrick J.D., Simons D.A., 1994, AJ 108, 437

Henry T.J., Ianna P.A., Kirkpatrick J.D., Jahreiss H., 1997, AJ 114, 388

Jones B.F., Fischer D.A., Stauffer J.R., 1996, AJ 112, 1562

Kirkpatrick J.D., Beichman C.A., Skrutskie M.F., 1997, ApJ 476, 311

Kroupa P., 1995, ApJ 453, 358

Leggett S.K., 1992, ApJS 82, 351

Leinert Ch., Jahreiss H., Haas M., 1986, A&A 164, L29

Leinert Ch., Haas M., Allard F., et al., 1990, A&A 236, 399

Leinert Ch., Henry T., Glindemann A., McCarthy Jr D. W., 1997, A&A 325, 159

McCaughrean M.J., Stauffer J.R., 1994, AJ 108, 1382

Marcy G.W., Lindsay V., Wilson K., 1987, PASP 99, 490

Marcy G.W., Benitz K.J., 1989, ApJ 344, 441

Marcy G.W., Butler R.P., Vogt S.S., Fischer D., Lissauer J.J., 1998, ApJ 505, L147

Mariotti J.M., Perrier C., Duquennoy A., et al., 1992, In: Beckers J.M., Merkle F. (eds.) High-Resolution Imaging by Interferometry II. European Southern Observatory, Garching bei München, Germany

Mayor M., Queloz D., 1995, Nat 378, 355

Nadeau D., Murphy D.C., Doyon R., Rowlands N., 1994, PASP 106, 909

Nakajima T., Durrance S.T., Golimovski D.A., Kulkarni S.R., 1994, ApJ 428, 797

Nakajima T., Oppenheimer B.R., Kulkarni S.R., et al., 1995, Nat 378, 463

Perrier, et al., 1999, in preparation for A&A

Pettersen B.R., Evans D.S., Coleman L.A., 1984, ApJ 282, 214

Queloz D., 1995a, Ph.D. Thesis 2788, University of Geneva

Queloz D., 1995b, In: Davis Philip A.G. (ed.) IAU Symposium 167, New developments in array technology and applications. Kluwer, Dordrecht, 221

Reid I.N., Hawley S.L., Gizis J.E., 1995, AJ 110, 1838

Reid I.N., Gizis J.E., 1997, AJ 113, 2246

Rigaut F., Arsenault R., Kerr J., et al., 1994, In: Ealey M.A., Merkle F. (eds.) SPIEE Proceedings 2201, Adaptive Optics in Astronomy. 149

Rigaut F., Salmon D., Arsenault R., et al., 1998, PASP 110, 152

Ritter H., Kolb U., 1998, A&AS 129, 83

Simons D.A., Henry T.J., Kirkpatrick J.D., 1996, AJ 112, 2238

Skrutskie M.F., Forrest W.J., Shure M., 1989, AJ 98, 1409

Tinney C.G., 1993, ApJ 414, 279

Tokovinin A.A., Ismailov R.M., 1988, A&AS 72, 563

Tokovinin A.A., 1992, A&A 256, 121

Tomkin J., Pettersen B.R., 1986, AJ 92, 1424

Udry S., Mayor M., Andersen J., et al., 1997, In: Proceedings of the ESA Symposium 'HIPPARCOS - Venice '97', ESASP-402, p. 693

Udry S., Mayor M., Queloz D., 1998, In: Hearnshaw J.B., Scarfe C.D. (eds.) Proceedings of IAU Colloquium 170, Precise stellar radial velocities. Victoria BC Canada, ASP Conference Series (1999), in press

Upgren A.R., Caruso J.R., 1988, AJ 96, 719

Upgren A.R., Harlow J.J.B, 1996, PASP 108, 64

Van Altena W.F., Lee J.T., Hoffleit D., 1995, The General Catalogue of Trigonometric Stellar Parallaxes. Fourth edition, Yale University Observatory (1995)

Véran J.-P., Rigaut F., Rouan D., Maitre H., 1997, J. Opt. Soc. Am. A 14(11), 3057

Young A., Sadjadi S., Harlan E., 1987, ApJ 314, 272